RESEARCH LETTER

Co-localization of particulate methane monooxygenase and cd_1 nitrite reductase in the denitrifying methanotroph '*Candidatus* Methylomirabilis oxyfera'

Ming L. Wu[1], Theo A. van Alen[1], Elly G. van Donselaar[2], Marc Strous[3,4], Mike S.M. Jetten[1] & Laura van Niftrik[1]

[1]Department of Microbiology, Institute for Water and Wetland Research, Radboud University Nijmegen, Nijmegen, The Netherlands; [2]Cellular Architecture & Dynamics, Utrecht University, Utrecht, The Netherlands; [3]MPI for Marine Microbiology, Bremen, Germany; and [4]Centre for Biotechnology, University of Bielefeld, Bielefeld, Germany

Correspondence: Mike S.M. Jetten, Department of Microbiology, Institute for Water and Wetland Research, Radboud University Nijmegen, Heyendaalseweg 135, 6525 AJ Nijmegen, The Netherlands. Tel.: +31 24 3652941; fax: +31 24 3652830; e-mail: m.jetten@science.ru.nl

Received 8 May 2012; revised 1 June 2012; accepted 3 June 2012.
Final version published online 22 June 2012.

DOI: 10.1111/j.1574-6968.2012.02615.x

Editor: J. Colin Murrell

Keywords
anaerobic methane oxidation; denitrification; *Methylomirabilis oxyfera*; intracellular immunogold localization; cd_1 nitrite reductase; particulate methane monooxygenase.

Abstract

'*Candidatus* Methylomirabilis oxyfera' is a polygon-shaped bacterium that was shown to have the unique ability to couple anaerobic methane oxidation to denitrification, through a newly discovered intra-aerobic pathway. Recently, the complete genome of *Methylomirabilis oxyfera* was assembled into a 2.7-Mb circular single chromosome by metagenomic sequencing. The genome of *M. oxyfera* revealed the full potential to perform both methane oxidation and the conversion of nitrite via nitric oxide into oxygen and dinitrogen gas. In this study, we show by immunogold localization that key enzymes from both methane- and nitrite-converting pathways are indeed present in single *M. oxyfera* cells. Antisera targeting the particulate methane monooxygenase (pMMO) and the cd_1 nitrite reductase (NirS) were raised and used for immunogold localization in both single- and double-labelling experiments. Our previous studies have shown that *M. oxyfera* does not develop pMMO-containing intracytoplasmic membranes as is observed in classical proteobacterial methanotrophs. Our results suggest that in *M. oxyfera*, the pMMO and NirS enzymes localized to the cytoplasmic membrane and periplasm, respectively. Further, double-labelling showed co-occurrence of pMMO and NirS in single *M. oxyfera* cells.

Introduction

The first evidence for the existence of anaerobic methane oxidation (AMO) coupled to denitrification was obtained with an enrichment culture from a Dutch canal sediment in 2006 (Raghoebarsing *et al.*, 2006). By that time, the co-culture was dominated (up to 80%) by one bacterial phylotype now named '*Candidatus* Methylomirabilis oxyfera' (Ettwig *et al.*, 2010) and a smaller fraction by a methanogenic archaeal species phylogenetically related to *Methanosaeta* and ANME-II. These and other observations led to the hypothesis of a mechanism involving two partners. In this mechanism, the archaea would drive the process through reverse methanogenesis and shuttle electrons to the denitrifying partner, in analogy to the consortia of sulphate-reducing bacteria and methanogenic archaea (Panganiban *et al.*, 1979; Knittel & Boetius, 2009). However, later, it was found that upon prolonged enrichment, the archaea disappeared from the culture, indicating that the complete process could be carried out by *Methylomirabilis oxyfera* alone (Ettwig *et al.*, 2008).

The genome of *M. oxyfera* was be assembled by a metagenomic sequencing approach of the total microbial community (Ettwig *et al.*, 2010). The genome of *M. oxyfera* contained all the necessary genes for methane oxidation, next to an unconventional denitrification pathway. When compared to the established route of denitrification, the pathway in *M. oxyfera* seemed to be 'truncated.' Notably, the genes encoding for the catalytic subunits of nitrous oxide reductase (Nos), the enzyme complex that converts nitrous oxide to dinitrogen gas, were not identified in the genome. Subsequently, by stable isotope

labelling studies, it was shown that besides dinitrogen gas, *M. oxyfera* also intra-aerobically produces oxygen from nitrite (Ettwig *et al.*, 2010). Following these experiments, it was proposed that *M. oxyfera* bypasses the nitrous oxide intermediate by direct disproportionation of nitric oxide into dinitrogen gas and oxygen (Ettwig *et al.*, 2010). Apart from the absence of the Nos enzyme, *M. oxyfera* transcribes and expresses the known enzymes for the reduction of nitrate to nitrite (nitrate reductase; Nar), nitrite to nitric oxide (cytochrome cd_1-type nitrite reductase; NirS) and nitric oxide to nitrous oxide (nitric oxide reductase; Nor). The physiological role of the Nor enzymes in *M. oxyfera* is still unclear. Because nitrous oxide is not an intermediate of *M. oxyfera*, the Nor enzymes might serve other purposes, such as NO detoxification or act as NO dismutases as suggested by Ettwig *et al.* (2010).

Prior to the discovery of *M. oxyfera*, methanotrophy was confined to specific groups within the classes of *Proteobacteria* and *Verrucomicrobia* (Trotsenko & Murrell, 2008; Op den Camp *et al.*, 2009). *Methylomirabilis oxyfera* is a member of the 'NC10' phylum, and thus, phylogenetically unrelated to the previously known methanotrophs (Raghoebarsing *et al.*, 2006; Wu *et al.*, 2011). Despite the phylogenetic position, *M. oxyfera* shares the enzymology of methane oxidation as described for the classical aerobic methanotrophs, that is, the oxidation of methane to carbon dioxide, via methanol, formaldehyde and formate. The first step of methane oxidation is mediated by methane monooxygenase (MMO) enzymes. Two forms of MMO enzymes are known, a cytoplasmic-soluble form (sMMO) and an integral membrane-bound particulate form (pMMO) (Hanson & Hanson, 1996; Brantner *et al.*, 2002; Trotsenko & Murrell, 2008). The latter appears to be a common feature among methanotrophs, and thus far, its absence has only been reported in *Methylocella palustris* strain KT (Dedysh *et al.*, 2000), which contains only sMMO. Some strains posses both pMMO and sMMO, and their differential expression can be influenced by growth conditions, such as copper availability (de Boer & Hazeu, 1972; Stanley *et al.*, 1983; Cornish *et al.*, 1985).

The pMMO is a metalloenzyme composed of three subunits, pMmoA (β), pMmoB (α) and pMmoC (γ), arranged in a trimeric $\alpha_3\beta_3\gamma_3$ complex (Lieberman & Rosenzweig, 2005). The roles of pMmoA and C subunits are not fully understood. However, the pMmoB domain has been shown to constitute the active site of the enzyme (Balasubramanian *et al.*, 2010). In the well-characterized proteobacterial methanotrophs, the expression of the pMMO enzyme complex is accompanied by the formation of extensive invaginations of the cytoplasmic membrane into intracytoplasmic membranes (ICM). Outside the *Proteobacteria*, it appears that ICM do not commonly occur. For instance, neither the Verrucomicrobial *Methylacidiphilum fumariolicum* strain SolV (Pol *et al.*, 2007) nor *M. oxyfera* possess ICM (Wu *et al.*, 2012).

To investigate whether both methane oxidation and nitrite conversion pathways are indeed present in *M. oxyfera*, we used single- and double-immunogold localization experiments to determine the intracellular location of both the pMMO and NirS enzymes.

Materials and methods

Methylomirabilis oxyfera enrichment culture

Methylomirabilis oxyfera was enriched and cultured in an anoxic sequencing batch reactor (15 L) at 30 °C on a mineral medium containing 20 mM nitrite and 3 mM nitrate as described elsewhere (Ettwig *et al.*, 2010). The medium was continuously sparged with a mixture of Ar/CO_2 (95 : 5 v/v) and CH_4/CO_2 (95 : 5 v/v, purity > 99.995%, Air Liquide, The Netherlands). *Methylomirabilis oxyfera* comprised about 70–80% of the population as previously shown by fluorescence *in situ* hybridization and metagenome analysis (Ettwig *et al.*, 2010; Luesken *et al.*, 2012). The residual community (about 20–30%) was highly diverse and evenly distributed over various phyla.

Analysis of the *M. oxyfera pmo* and *nirS* gene clusters

Sequences of the *pmo* and *nirS* gene clusters were retrieved from the *M. oxyfera* genome available under GenBank accession number FP565575. Transmembrane protein topology was predicted using the TMHMM program (Krogh *et al.*, 2001) (http://www.cbs.dtu.dk/services/TMHMM-2.0/). The prediction of the signal peptide was performed using the SIGNAL P tool (Petersen *et al.*, 2011) (http://www.cbs.dtu.dk/services/SignalP/) using a hidden Markov model and Gram-negative trained models.

Antisera production

The antisera target regions were selected on the basis of minimal sequence similarity to other proteins using the BLAST alignment tool. Polyclonal antiserum against the *M. oxyfera* and NirS enzyme was raised by injecting rabbits with two synthetic peptides: peptide 1 (amino acid position 139–153: PPDKRPTKPEHNRDW) and peptide 2 (amino acid position 520–534: EKARIDDPRIITPTG). Prior to the immunization, an extra amino-terminal cysteine was added to the peptide sequences for the conjugation to the Keyhole limpet haemocyanin (Eurogentec, Belgium).

For the *M. oxyfera* pMMO enzyme, two polyclonal antisera targeting α-subunit (pMmoB) were raised.

α-pMmoB1 was raised by injection of rabbits with two synthetic peptides: peptide 1 (amino acid position 257–271: QTGRMDTPELKPTTE) and peptide 2 (amino acid position 324–337: DPALFPDSRLKIKVE). Prior to the immunization, an extra amino-terminal cysteine was added to the peptide sequences for the conjugation to the Keyhole limpet haemocyanin (Eurogentec). α-pMmoB2 was generated from a heterologously expressed and purified fragment of *pmoB* in *Escherichia coli* as described previously (Harhangi *et al.*, 2002), with the following modifications. Two primers were designed on the *pmoB* sequence; a forward primer on nucleotide position 790 (CCCGAACTGAAGCCCACGACAGAG) and a reverse primer on nucleotide position 1188 (GCCGCCGACCTCAACAATTTGTCTG). A stop codon (TAA) was included in the reverse primer so as to express only an N-terminal His-tag. For directional cloning, restriction sites EcoRI and NotI were included in the forward primer and XhoI in the reverse primer. An additional nucleotide (T) was added between EcoRI and NotI so as to bring the sequence in frame. pET-30a(+) (Novagen, Germany) was used as the expression vector. Rosetta cells (Novagen) were used as the expression host. The heterologously expressed protein fragment (amino acid position 264–396) was purified using the HIS-Select® HF nickel affinity gel column (Sigma, The Netherlands) under denaturing conditions using the protocol provided by the manufacturer. The identity of the expressed protein fragment was verified by MALDI-TOF MS peptide mass fingerprinting of a tryptic digest of the purified protein fragment (Harhangi *et al.*, 2002).

For each antiserum, two rabbits were immunized using a 3-month immunization protocol. The antisera from both rabbits were pooled and affinity-purified (Eurogentec). The affinity-purified antisera (α-NirS, α-pMmoB1 and α-pMmoB2) were used as the primary antisera in immunoblot analysis and immunogold localization as described later.

Preparation of whole-cell extracts of *M. oxyfera*

Approximately 2 g of cells (wet weight) was taken from the *M. oxyfera* enrichment culture. The cells were washed three times with 20 mM phosphate buffer pH 8.0 and resuspended in a medium containing 20 mM sodium phosphate and 50 mM sodium pyrophosphate pH 8.0. Cells were broken by sonication. Cell debris was removed by centrifugation (6000 ***g***, 15 min, 4 °C), and the supernatant was collected as whole-cell extract. Protein content of the samples was determined by the Bradford method (Bradford, 1976) using a Bio-Rad protein assay kit (Bio-Rad, Veenendaal, The Netherlands) with BSA as standard.

SDS-PAGE and immunoblot analysis

Methylomirabilis oxyfera whole-cell extracts were separated (30 μg of protein per lane) on a 10% SDS-PAGE gel and transferred to a nitrocellulose membrane (Protran®, Germany) with a semi-dry transfer cell blotting system (Bio-Rad). Blotting was performed at 100 mA for 45 min with a transfer buffer containing 25 mM Tris, 192 mM glycine and 20% methanol. After blotting, the blots were air-dried and stored at 4 °C until further use.

For immunoblotting, the stored blots were washed in distilled water for 30 min. Subsequently, the blots were (1) incubated in blocking buffer (1% BSA) in Tris-buffered saline (TBS; 10 mM Tris-HCL, 0.9% NaCl, pH 7.4) for 1 h; (2) incubated for 1 h in either blocking buffer or rabbit preimmune serum diluted 250-fold in blocking buffer (negative controls) or antiserum diluted 250-fold in blocking buffer; (3) washed tree times for 10 min in TBS containing 0.05% Tween20; (4) incubated for 1 h in monoclonal mouse α-rabbit IgG alkaline phosphatase conjugate (γ-chain specific; Sigma, The Netherlands) diluted 1500-fold in blocking buffer; (5) washed two times for 10 min in TBS containing 0.05% Tween and three times for 10 min in TBS; and (6) incubated for 5 min in alkaline phosphatase substrate BCIP/NBT (Sigma), rinsed in distilled water and air-dried.

Sample preparation for immunogold localization: chemical fixation and cryosectioning [Tokuyasu technique (Tokuyasu, 1973)]

Cells from the *M. oxyfera* enrichment culture were chemically fixed by immersion in 2% paraformaldehyde and 0.2% glutaraldehyde in 0.1 M PHEM buffer (25 mM HEPES, 10 mM EGTA, 60 mM PIPES, 2 mM $MgCl_2$, pH 6.9) for 1 h, at room temperature, followed by overnight fixation at 4 °C. Next, the samples were washed three times with 0.1 M PHEM buffer pH 6.9 and resuspended in 12% gelatin in 0.1 M PHEM buffer pH 6.9 at 37 °C. After 5 min at 37 °C, the samples were pelleted by a centrifugation step, half of the supernatant was removed, and the samples were placed on ice for 15 min. The gelatin-embedded cells were cut into small cubes (1–2 mm^3) under a stereo microscope, infiltrated overnight in rotating vials at 4 °C with 2.3 M sucrose in 0.1 M PHEM buffer pH 6.9 and frozen in liquid nitrogen. Cryosectioning was performed in a cryoultramicrotome (UCT/FCS or UC6/FCS; Leica Microsystems, Vienna, Austria). Ultrathin cryosections (about 70-nm) were picked up with a drop of 1% methylcellulose and 1.15 M sucrose in PHEM buffer and transferred to carbon-formvar-coated grids (copper, hexagonal 100-mesh) for immunogold localization.

Immunogold localization

For single labelling, grids containing ultrathin sections of *M. oxyfera* cells were (1) washed for 30 min at 37 °C with PBS; (2) incubated for 10 min on drops of PBS containing 20 mM glycine and blocked for 20 min on drops of PBS containing 1% BSA or 1% skim milk powder (Frema Reform, Germany); (3) incubated for 1 h with or without (negative control) the primary antiserum diluted 20- or 50-fold in PBS containing 1% BSA or 1% skim milk powder; (4) washed for 12 min on drops of PBS containing 0.1% BSA or 0.1% skim milk powder; (5) incubated for 20 min with protein A coupled to 5 or 10 nm gold (PAG5 or PAG10, CMC/UMC, Utrecht, The Netherlands), diluted 70-fold in PBS containing 1% BSA or 1% skim milk powder; (6) washed for 14 min on drops of PBS; (7) fixed for 5 min with PBS containing 1% glutaraldehyde and washed for 10 min on drops of distilled water; (8) poststained for 5 min with 2% Uranyl acetate in 0.15 M oxalic acid (pH 7.4) and washed quickly on two drops of distilled water and then on two drops of 1.8% methyl cellulose containing 0.4% aqueous uranyl acetate on ice; and (9) embedded for 5 min in 1.8% methylcellulose containing 0.4% aqueous uranyl acetate on ice after which they were air-dried.

For double-labelling, the labelling with each antiserum was discriminated by applying different sizes, 5 and 10 nm, of protein A–coupled gold particles (PAG5 and PAG10, respectively). Labelling of the second antiserum was performed by repeating the steps 2–7 from the single-labelling protocol described earlier.

Transmission electron microscopy (TEM)

Grids containing ultrathin cryosections of *M. oxyfera* cells were investigated in a transmission electron microscope at 60 or 80 kV (Tecnai12; FEI Company, Eindhoven, The Netherlands). Images were recorded using a CCD camera (MegaView II, AnalySis).

Results

nirS and *pmo* gene clusters in *M. oxyfera*

In all the enrichment cultures described so far, nitrite is preferred over nitrate as electron acceptor (Wu *et al.*, 2011). The reduction of nitrite to nitric oxide is catalysed by nitrite reductases (Nir). Two types of NO-producing nitrite reductase enzymes have been identified so far: the copper-containing type and the cytochrome cd_1 type (Zumft, 1997). In *M. oxyfera*, only the latter is present and is encoded by the *nirSJFD/GH/L* operon (Fig. 1a). In all the translated sequences, an N-terminal signal sequence for membrane translocation was found, suggesting their periplasmic localization in the cell. The *nirJ*, *nirF* and the fused *nirD/GH/L* genes encode proteins consisting of 384, 409 and 406 amino acids, respectively. In other cd_1-type NirS-containing denitrifiers, these genes have been shown to be required for biosynthesis and maturation of the heme d_1 (Zumft, 1997). The *nirS* gene encodes the structural NirS protein. The calculated molecular mass of the gene product from *M. oxyfera* for *nirS* (546 amino acids) without the peptide sequence is 58.2 kDa.

The genome of *M. oxyfera* contains one set of *pmoCAB* genes encoding the membrane-bound form of the MMO enzyme (Fig. 1b). Genes encoding the soluble form are absent (Ettwig *et al.*, 2010). Upstream, the gene cluster contains an additional copy of the *pmoC* (*pmoC2*) gene that is 100% identical to *pmoC1* at the nucleotide level. The translated protein sequences of the *pmoCAB* genes have a calculated molecular mass of 28.3, 30.0 and 44.2 kDa, respectively. The translated sequence of the *pmoB* extramembrane subunit has an N-terminal signal sequence of 25 amino acids involved in membrane translocation.

Antisera specificity

Synthetic peptides were used to generate specific primary antisera against the *M. oxyfera* NirS (α-NirS) and pMMO (α-pMmoB1) in rabbits. We additionally cloned and heterologously expressed a fragment of *pmoB* in *E. coli* and used the expressed fragment to raise antiserum (α-pMmoB2). All antisera were affinity-purified and their specificity was tested on whole-cell extract of the *M. oxyfera* enrichment culture using SDS-PAGE and immunoblot analysis.

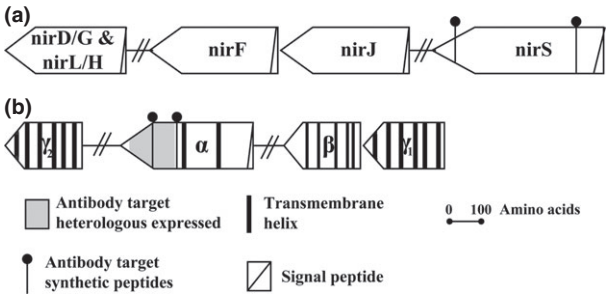

Fig. 1. Physical map of the *pmo* and *nirS* gene clusters in *Methylomirabilis oxyfera* and the target positions of the antisera. (a) *Methylomirabilis oxyfera nirS* gene cluster [ORF identifiers (from left to right): DAMO_2409, DAMO_2412, DAMO_2413 and DAMO_2415]. (b) *Methylomirabilis oxyfera pmo* gene cluster [ORF identifiers (from left to right): DAMO_2339, DAMO 2448, DAMO_2450 and DAMO_2451]. The arrows indicate the direction of transcription.

Incubations with the antiserum targeting NirS showed a band of approximately the expected size (58.2 kDa; Fig. 2, lane 6). No bands were detected in blots incubated with blocking buffer or preimmune serum instead of the antiserum (negative controls; data not shown). For the antisera against pMMO, both α-pMmoB1 and α-pMmoB2 showed a band of about the expected size (44.2 kDa; Fig. 2, lanes 2 and 4), which were absent when incubated with either blocking buffer or preimmune serum instead of the antiserum (negative controls; data not shown). When using the same antisera dilutions, a stronger signal was observed when using α-pMmoB2 compared to α-pMmoB1.

These results showed that the derived antisera were specific for the targeted proteins and provide a reliable basis for immunogold localization of the enzymes in ultrathin sections of *M. oxyfera* cells.

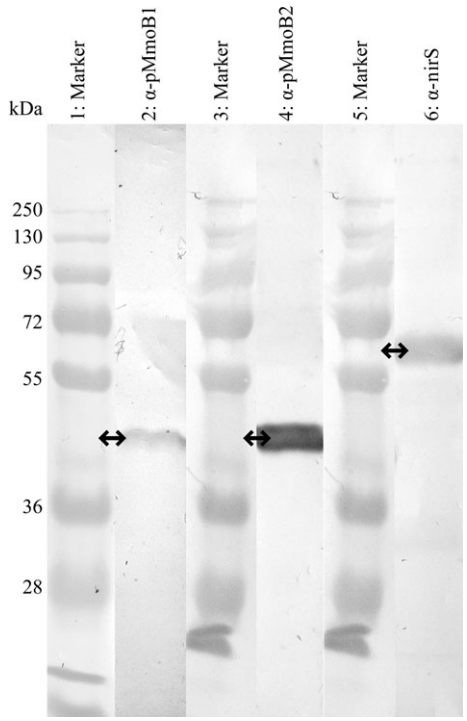

Fig. 2. Immunoblot analysis of the affinity-purified antisera targeting the pMMO and NirS of *Methylomirabilis oxyfera,* showing specific binding to proteins of the expected size. The 10% SDS-PAGE gels were loaded with 30 μg protein/lane (*M. oxyfera* whole-cell extracts) and blotted onto a nitrocellulose membrane. Lanes 1, 3 and 5, markers (PageRuler Prestained Ladder Plus; Fermentas, Germany). Lane 2, incubation with antiserum targeting 15 amino acids of pMmoB that was raised using synthetic peptides (α-pMmoB1). Lane 4, incubation with antiserum targeting 132 amino acids of pMmoB that was heterologously expressed in *Escherichia coli* (α-pMmoB2). Lane 6, incubation with antiserum targeting 15 amino acids of NirS that was raised using synthetic peptides (α-NirS).

Immunolocalization of pMMO in *M. oxyfera*

Cells from the *M. oxyfera* enrichment culture were chemically fixed and cryosectioned. *Methylomirabilis oxyfera* cells could be distinguished from other cells of the community by their polygonal cell shape (Wu *et al.*, 2012). The identity of the polygon-shaped cells to *M. oxyfera* has been confirmed previously by fluorescence *in situ* hybridization (FISH) using 'NC10' bacteria-specific probes (Wu *et al.*, 2012). As in our previous study, the polygon-shaped *M. oxyfera* cells lacked ICM and the configuration of the cytoplasmic membrane was predominantly smooth and devoid of invaginations (Fig. 3). Cells from the other community members were morphologically diverse.

The negative control where ultrathin sections of *M. oxyfera* cells were incubated with PAG5 or PAG10 alone showed no background labelling (data not shown). Likewise, cross-reactivity of the affinity-purified antisera with other cells was not detected. In the incubations with α-pMmoB1 or α-pMmoB2, only *M. oxyfera* cells were specifically labelled. The gold particles occurred at or close to the cytoplasmic membrane (Fig. 3). As for immunoblot analysis, more labelling was observed when using α-pMmoB2 compared to α-pMmoB1 when using the same antisera dilutions.

Immunolocalization of NirS in *M. oxyfera*

Ultrathin cryosections of *M. oxyfera* cells were incubated with α-NirS for the determination of the intracellular location of this enzyme. Labelling was observed only in the polygon-shaped *M. oxyfera* cells (Fig. 4). The negative control where ultrathin sections of *M. oxyfera* cells were incubated with PAG5 or PAG10 alone showed no background labelling (data not shown). Likewise, cross-reactivity of the affinity-purified antiserum with other cells was not detected. The NirS labelling was mostly confined to the vicinity of the cytoplasmic membrane of *M. oxyfera* cells. Occasionally, some gold particles were detected inside the cytoplasm.

Co-immunolocalization of NirS and pMMO in *M. oxyfera*

We used double-labelling to co-localize pMMO and NirS in single *M. oxyfera* cells. Because α-pMmoB2 worked best in the single-labelling experiments, we used this antiserum in combination with α-NirS for co-localization. Gold particles of each antiserum could be discriminated using protein A gold (PAG) with gold particles of different sizes (PAG5 and PAG10; 5 and 10 nm, respectively). Figure 5 shows the ultrathin sections of *M. oxyfera* cells

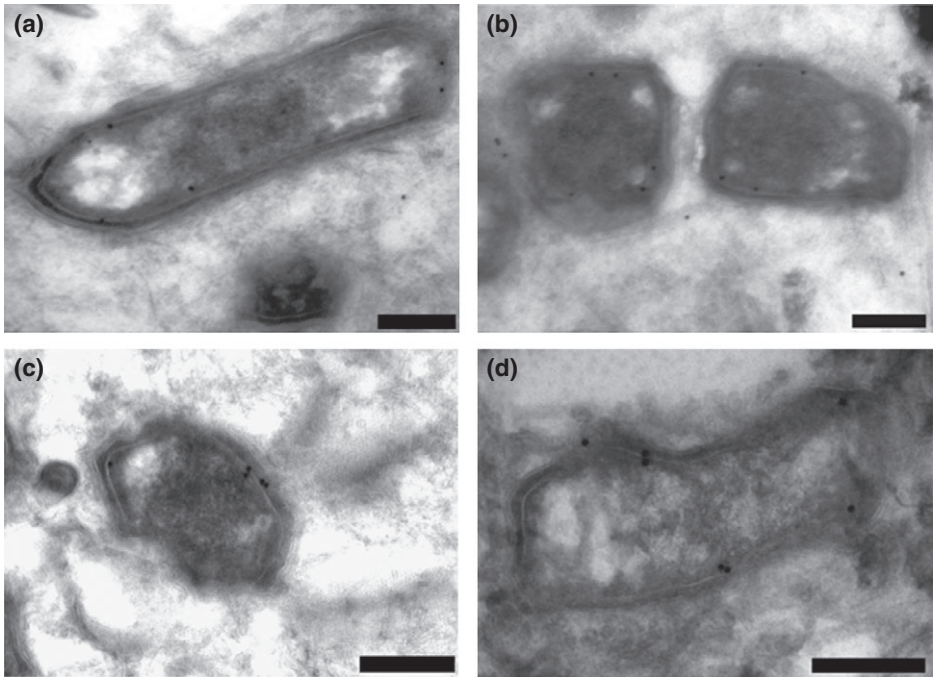

Fig. 3. Transmission electron micrographs of chemically fixed and cryosectioned *Methylomirabilis oxyfera* cells showing immunogold localization of the affinity-purified antisera directed against pMMO (α-pMmoB1 and α-pMmoB2). Sections were blocked with 1% skim milk powder and treated with 20-fold diluted α-pMmoB1 that was raised using synthetic peptides (a, b) and blocked with 1% BSA and treated with 20-fold diluted α-pMmoB2 that was heterologously expressed in *Escherichia coli* (c, d). Scale bars, 200 nm.

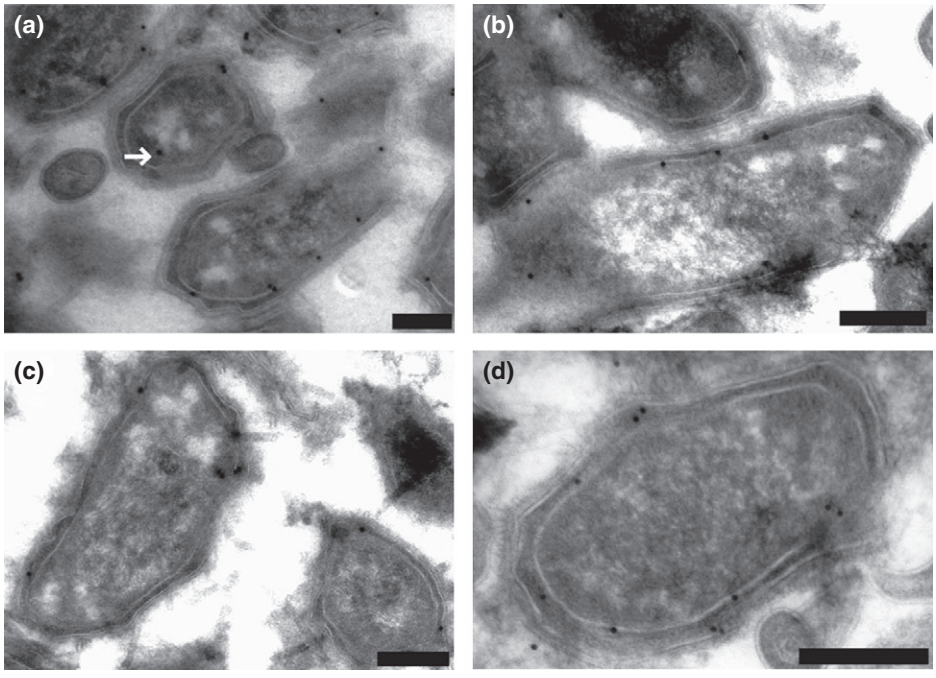

Fig. 4. Transmission electron micrographs of chemically fixed and cryosectioned *Methylomirabilis oxyfera* cells showing immunogold localization of the affinity-purified antiserum directed against NirS (α-NirS) that was raised using synthetic peptides. Sections were blocked with 1% BSA and treated with 50-fold diluted α-NirS (a) or 1% skim milk powder and treated with 20-fold diluted α-NirS (b–d). White arrow shows a gold particle inside the cytoplasm. Scale bars, 200 nm.

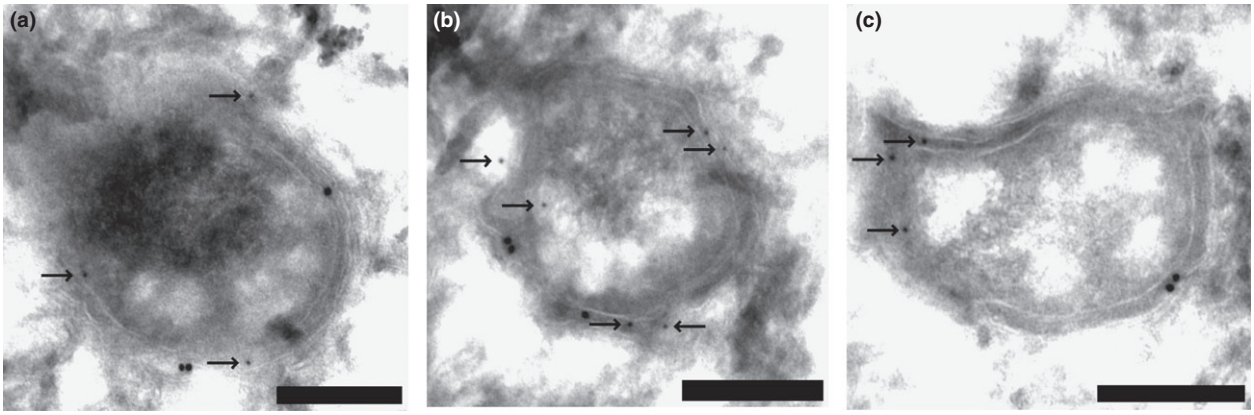

Fig. 5. Transmission electron micrographs of chemically fixed and cryosectioned *Methylomirabilis oxyfera* cells showing co-localization of the antisera directed against NirS (α-NirS: smaller, 5 nm, gold particles; arrows) and pMmoB (α-pMmoB2: larger, 10 nm, gold particles) (a-c). Sections were blocked with 1% BSA and treated with 20-fold diluted α-pMmoB2 that was raised using a heterologously expressed protein in *Escherichia coli*, followed by blocking with 1% skim milk powder and treatment with 20-fold diluted α-NirS that was raised using synthetic peptides. Scale bars, 200 nm.

incubated with α-pMmoB2 and α-NirS antisera and their respective co-localization in the polygon-shaped *M. oxyfera* cells. Similar to the single labelling, both NirS and pMMO were found in vicinity or at the cytoplasmic membrane of *M. oxyfera*.

Discussion

'*Candidatus* Methylomirabilis oxyfera' is thus far the only known organism capable of performing the process of AMO coupled to nitrite reduction (Ettwig *et al.*, 2010; Wu *et al.*, 2011). The ability to perform the AMO process has been demonstrated in various enrichment cultures and is corroborated by *in silico* analysis of the genome of *M. oxyfera* assembled from a mixed microbial community (Ettwig *et al.*, 2010; Wu *et al.*, 2011). Here, we investigated whether key enzymes of the methane- and nitrite-converting pathways are indeed present in single *M. oxyfera* cells. Antisera targeting pMMO and cd_1-type NirS (Fig. 1) were derived and used in immunogold labelling. By immunoblot analysis of *M. oxyfera* whole-cell extracts, we confirmed the specificity of the antisera and the absence of cross-reactivity (Fig. 2). Immunogold localization further showed the presence of both enzymes in *M. oxyfera* cells in both single- and double-labelling experiments (Figs 3–5).

Ultrathin sections of *M. oxyfera* cells incubated with α-NirS showed NirS to be present in the vicinity of the cytoplasmic membrane of *M. oxyfera* cells (Figs 3 and 5). This localization is in agreement with a periplasmic protein. Gold particles are often observed at some distance from the actual localization of the protein due the size of antigen–PAG complex (about 25 nm). The immunolabelling results taken together with the presence of an amino-terminal signal sequence for membrane translocation in the *M. oxyfera* nirS sequence (Fig. 1a) strongly suggest that NirS is present in the periplasm of *M. oxyfera* cells, like in other denitrifying bacteria (Zumft, 1997). Occasionally, a few colloidal gold particles were observed inside the cytoplasm of *M. oxyfera* cells (Fig. 4, white arrow). This could be due to the presence of precursor protein, which is present in the cytoplasm before export to the periplasmic space.

One of the characteristic features of methanotrophs is the presence of ICM. In aerobic proteobacterial methanotrophs, pMMO is found physically embedded in these structures. ICM occur in two main arrangements: vesicular stacks (type I; γ-proteobacterial methanotrophs) and pairs of peripheral layers located parallel to the cell envelope (type II; α-proteobacterial methanotrophs) (Hanson & Hanson, 1996; Trotsenko & Murrell, 2008). In our previous study on the ultrastructure of *M. oxyfera*, neither TEM nor electron tomography showed the presence of ICM in *M. oxyfera* cells under the current growth conditions (Wu *et al.*, 2012). This observation raised the question regarding the actual intracellular location of the pMMO enzyme in *M. oxyfera*. Here, we show that, consistent with the previous observation, *M. oxyfera* does not develop ICM under the current growth conditions. Ultrathin section of *M. oxyfera* cells incubated with α-pMmoB showed gold particles both at and close to the cytoplasmic membrane (Figs 4 and 5). These results together with the presence of membrane spanning regions in the pMmoB sequence (Fig. 1b) indicate that the pMMO enzyme is most likely located at the cytoplasmic membrane of *M. oxyfera* cells.

In conclusion, our results suggest that pMMO and NirS enzymes are located in the cytoplasmic membrane and the periplasm of *M. oxyfera* cells, respectively. Double-labelling experiments showed the co-occurrence of

both pMMO and NirS in single *M. oxyfera* cells. Our results validate the presence of key enzymes in methane- and nitrite-converting pathways in the *M. oxyfera* metagenome assembly.

Acknowledgements

We would like to thank Katinka van de Pas-Schoonen for support in maintaining the *M. oxyfera* enrichment culture, Harry R. Harhangi, Huub Op den Camp and Jan T. Keltjens for stimulating discussions, Sarah Neumann for support in the production of the antisera and Geert-Jan Janssen for support at the general instruments facility. L.v.N. is supported by the Netherlands Organization for Scientific Research (VENI grant 863.09.009), M.L.W. by a Horizon grant (050-71-058), M.S. by ERC 242635 and M.S.M.J. by ERC 232937.

References

Balasubramanian R, Smith SM, Rawat S, Yatsunyk LA, Stemmler TL & Rosenzweig AC (2010) Oxidation of methane by a biological dicopper centre. *Nature* **465**: 115–119.

Bradford MM (1976) A rapid and sensitive method for the quantitation of microgram quantities of protein utilizing the principle of protein-dye binding. *Anal Biochem* **72**: 248–254.

Brantner CA, Remsen CC, Owen HA, Buchholz LA & Collins MLP (2002) Intracellular localization of the particulate methane monooxygenase and methanol dehydrogenase in *Methylomicrobium album* BG8. *Arch Microbiol* **178**: 59–64.

Cornish A, MacDonald J, Burrows KJ, King TS, Scott D & Higgins IJ (1985) Succinate as an *in vitro* electron donor for the particulate methane mono-oxygenase of *Methylosinus trichosporium* OB3b. *Biotechnol Lett* **7**: 319–324.

de Boer WE & Hazeu W (1972) Observations on the fine structure of a methane-oxidizing bacterium. *Antonie Van Leeuwenhoek* **38**: 33–47.

Dedysh SN, Liesack W, Khmelenina VN, Suzina NE, Trotsenko YA, Semrau JD, Bares AM, Panikov NS & Tiedje JM (2000) *Methylocella palustris* gen. nov., sp nov., a new methane-oxidizing acidophilic bacterium from peat bags, representing a novel subtype of serine-pathway methanotrophs. *Int J Syst Evol Microbiol* **50**: 955–969.

Ettwig KF, Shima S, van de Pas-Schoonen KT, Kahnt J, Medema MH, Op den Camp HJM, Jetten MSM & Strous M (2008) Denitrifying bacteria anaerobically oxidize methane in the absence of Archaea. *Environ Microbiol* **10**: 3164–3173.

Ettwig KF, Butler MK, Le Paslier D *et al.* (2010) Nitrite-driven anaerobic methane oxidation by oxygenic bacteria. *Nature* **464**: 543–548.

Hanson RS & Hanson TE (1996) Methanotrophic bacteria. *Microbiol Rev* **60**: 439–471.

Harhangi HR, Steenbakkers PJM, Akhmanova A, Jetten MSM, van der Drift C & Op den Camp HJM (2002) A highly expressed family 1 beta-glucosidase with transglycosylation capacity from the anaerobic fungus *Piromyces* sp. E2. *Biochim Biophys Acta* **1574**: 293–303.

Knittel K & Boetius A (2009) Anaerobic oxidation of methane: progress with an unknown process. *Annu Rev Microbiol* **63**: 311–334.

Krogh A, Larsson B, von Heijne G & Sonnhammer ELL (2001) Predicting transmembrane protein topology with a hidden Markov model: application to complete genomes. *J Mol Biol* **305**: 567–580.

Lieberman RL & Rosenzweig AC (2005) Crystal structure of a membrane-bound metalloenzyme that catalyses the biological oxidation of methane. *Nature* **434**: 177–182.

Luesken FA, Wu ML, Op den Camp HJM, Keltjens KT, Stunnenberg H, Francoijs KJ, Strous M & Jetten MSM (2012) Effect of oxygen on the anaerobic methanotroph '*Candidatus* Methylomirabilis oxyfera:' kinetic and transcriptional analysis. *Environ Microbiol* **14**: 1024–1034.

Op den Camp HJM, Islam T, Stott MB, Harhangi HR, Hynes A, Schouten S, Jetten MSM, Birkeland NK, Pol A & Dunfield PF (2009) Environmental, genomic and taxonomic perspectives on methanotrophic *Verrucomicrobia*. *Environ Microbiol Rep* **1**: 293–306.

Panganiban AT, Patt TE, Hart W & Hanson RS (1979) Oxidation of methane in the absence of oxygen in lake water samples. *Appl Environ Microbiol* **37**: 303–309.

Petersen TN, Brunak S, von Heijne G & Nielsen H (2011) SignalP 4.0: discriminating signal peptides from transmembrane regions. *Nat Methods* **8**: 785–786.

Pol A, Heijmans K, Harhangi HR, Tedesco D, Jetten MSM & Op den Camp HJM (2007) Methanotrophy below pH 1 by a new Verrucomicrobia species. *Nature* **450**: 874–878.

Raghoebarsing AA, Pol A, van de Pas-Schoonen KT *et al.* (2006) A microbial consortium couples anaerobic methane oxidation to denitrification. *Nature* **440**: 918–921.

Stanley SH, Prior SD, Leak DJ & Dalton H (1983) Copper stress underlies the fundamental change in intracellular location of methane mono-oxygenase in methane oxidizing organisms – studies in batch and continuous cultures. *Biotechnol Lett* **5**: 487–492.

Tokuyasu KT (1973) A technique for ultramicrotomy of cell suspensions and tissues. *J Cell Biol* **57**: 551–565.

Trotsenko YA & Murrell JC (2008) Metabolic aspects of aerobic obligate methanotrophy. *Adv Appl Microbiol* **63**: 183–229.

Wu ML, Ettwig KF, Jetten MSM, Strous M, Keltjens JT & van Niftrik L (2011) A new intra-aerobic metabolism in the nitrite-dependent anaerobic methane-oxidizing bacterium *Candidatus* 'Methylomirabilis oxyfera'. *Biochem Soc Trans* **39**: 243–248.

Wu ML, van Teeseling MCF, Willems MJR, van Donselaar EG, Klingl A, Rachel R, Geerts WJC, Jetten MSM, Strous M & van Niftrik L (2012) Ultrastructure of the denitrifying methanotroph '*Candidatus* Methylomirabilis oxyfera': a novel polygon-shaped bacterium. *J Bacteriol* **194**: 284–291.

Zumft WG (1997) Cell biology and molecular basis of denitrification. *Microbiol Mol Biol Rev* **61**: 533–616.